



Understanding transparent exopolymer particle occurrence and interaction with algae, bacteria, and the fractions of natural organic matter in the Red Sea: implications for seawater desalination

Abdullah H.A. Dehwah^{a,b}, Donald M. Anderson^c, Sheng Li^{a,d,e}, Francis L. Mallon^f, Zenon Batang^f, Abdullah H. Alshahri^a, Seneshaw Tsegaye^g, Michael Hegy^h, Thomas M. Missimer^{h,*}

^aWater Desalination and Reuse Center (WDRC), Biological and Environmental Science and Engineering (BESE), King Abdullah University of Science and Technology (KAUST), Thuwal 23955-6900, Saudi Arabia

^bDesalination Technologies Research Institute (DTRI), Saline Water Conversion Corporation (SWCC), P.O. Box: 8328, Al-Jubail 31951, Saudi Arabia

^cBiology Department, Woods Hole Oceanographic Institution, Woods Hole, MA 02543, USA

^dGuangzhou Institute of Advanced Technology, CAS, Haibin Road #1121, Nansha District, Guangzhou 511458, China

^eQingdao Yonglixing Water Purification Technology Ltd. Company, Room 605, Building B, Miaoling Road #36, Laoshan District, Qingdao, China

^fCoastal and Marine Resources Core Laboratory, King Abdullah University of Science and Technology (KAUST), Thuwal 23955-6900, Saudi Arabia

^gDepartment of Environmental and Civil Engineering, U.A. Whitake College of Engineering, 10501 FGCU Boulevard, Fort Myers, FL 33965-6565, USA

^hEmergent Technologies Institute, U.A. Whitaker College of Engineering, 16301 Innovation Lane, Fort Myers, FL 33913, USA, email: tmissimer@fgcu.edu (T.M. Missimer)

Received 19 February 2020; Accepted 7 April 2020

ABSTRACT

Binding of particulate and dissolved organic matter in the water column by marine gels allows the sinking and cycling of organic matter into the deeper water of the Red Sea and other marine water bodies. A series of four offshore profiles were made at which concentrations of bacteria, algae, particulate transparent exopolymer particles (p-TEP), colloidal transparent exopolymer particles (c-TEP), and the fractions of natural organic matter (NOM), including biopolymers, humic substances, building blocks, low molecular weight (LMW) neutrals, and LMW acids were measured to depths ranging from 90 to 300 m. It was found that a statistically-significant relationship occurs between the concentrations of p-TEP with bacteria and algae, but not with total organic carbon (TOC) in the offshore profiles. Variation in the biopolymer fraction of NOM in relationship to TEP and bacteria suggests that extracellular discharges of polysaccharides and proteins from the bacteria and algae are occurring without immediate abiotic assembly into p-TEP. In the water column below the photic zone, TOC, bacteria, and biopolymers show a generally common rate of reduction in concentration, but p-TEP decreases at a diminished rate, showing that it persists in moving organic carbon deeper into the water column despite consumption by bacteria. The data presented herein are the first to link TEP concentrations in the Red Sea with the fractions of NOM as measured using liquid chromatography organic carbon detection (LCOCD) technology. The oceanographic and water quality investigations show the seawater used for reverse osmosis desalination from the nearshore or offshore would yield nearly equal treatment challenges. Use of deep water intake systems to obtain seawater with reduced p-TEP and bacteria concentrations would not significantly impact treatment if it would be feasible which is not.

Keywords: Transparent exopolymer particles; Natural organic matter; Biofouling; Red Sea; Seawater reverse osmosis desalination

* Corresponding author.

1. Introduction

Biofouling potential for reverse osmosis seawater desalination (SWRO) plants is related to the biogeochemistry of the feedwater [1–4]. The role of transparent exopolymer particles (TEP) as a membrane preconditioning substance that accelerates biofouling has been documented [5–8]. Therefore, it is important for SWRO design engineers and microbiologists to better understand the biogeochemical processes in the sea that impact the creation and degradation of TEP. A significant quantity of data on TEP and its relationship to marine bacteria and other organic carbon compounds has been collected in the Red Sea [9–18]. It is the purpose of this research to document what is known about TEP formation and its relationship to other organic carbon forms and the general marine chemistry of the Red Sea.

Mechanisms that control the biogeochemical cycles influenced by microorganisms in the world's oceans are complex and poorly understood [19]. The relationships between microalgal and bacterial abundance, total organic carbon (TOC), fractions of natural organic matter (NOM), polysaccharides, and TEP in seawater with depth play important roles in the transport and cycling of nutrients and particulate organic matter (POM) in general [19–22]. In particular, the binding of suspended sediments and POM by TEP and other acidic polysaccharides, in addition to general aggradation, tends to increase particle size and weight, thus increasing settling rates in the water column [23,24]. It has been demonstrated that gel-type particles link particulate and dissolved organic matter in the ocean [25]. The sinking of biogenic particles drives elemental cycling, which in turn controls primary and secondary productivity through the water column [23]. Particulate organic material is commonly occupied or influenced by bacteria which can reduce the biomass by consumption of organic matter over various timeframes from days to weeks [25].

TEP are ubiquitous in the oceans [21], likely formed by abiotic coagulation and aggradation of dissolved carbohydrates or primarily acidic polysaccharides, but also by biotic formation as extracellular secretions by algae and bacteria [22,26–29]. Particulate TEP (p-TEP) is in the size range 0.4–200 μm , with a number of forms, including amorphous blobs, disseminated clouds, sheets, filaments, or clumps [21,30,31]. Colloidal TEP (c-TEP) consist of particles that are stained by Alcian blue with a diameter range of 0.05–0.4 μm [6]. However, c-TEP is defined based solely on staining with Alcian blue, which is known to also stain other substances in seawater, including sulfated and carboxylated polysaccharides, glycoproteins, polyanions in general, and acidic polysaccharides not associated with TEP [4].

TEP are composed of acidic polysaccharides enriched with fucose and rhamnose, thus serving as a food source in the water column and commonly associated with layers of intense microbial and biochemical activity [32]. TEP generally decrease in concentration with depth in the sea [33], with a tendency to float to the sea surface if unbalanced to contribute a gelatinous layer to the sea surface microlayer [34–36]. Bar-Zeev et al. [8] have documented that p-TEP is mainly composed of polysaccharides, which can be dispersed in the presence of different types of chelators, be fractured to form colloids or reassemble abiotically.

The trends in TEP concentrations in the seawater column have been previously examined [37], and the relationship of TEP with TOC, dissolved organic carbon (DOC), and bacteria have also been investigated in many areas of the ocean [38–43]. However, these relationships have not been studied in the Red Sea.

Studies on TEP distribution in relation to other forms of organic matter in the Red Sea have focused mainly on assessing the links between TEP and phytoplankton and bacterial production [44] and the impacts of TEP and dissolved forms of NOM on biofouling in seawater desalination plants [9–18,45]. The intakes for SWRO plants are located in shallow, nearshore areas of the Red Sea, so little consideration has been given to changes in TEP concentration with depth until it was suggested that deep-water intake systems may produce seawater quality with lower concentrations of algae, bacteria, and organic compounds, such as TEP, thus possibly lessening rates of membrane biofouling [11].

The relationships between TEP concentrations and abundance of microalgae, bacteria, TOC, and dissolved fractions of NOM, including biopolymers, humic substances, building blocks, low molecular weight (LMW) acids, and LMW neutrals from the sea surface to 300 m depth are herein presented. The present study provides the first data from the Red Sea, with initial insights into the vertical transport of organic carbon, including the fractions of NOM from the surface to depths near or below the photic zone. The authors are keenly aware that the data presented herein have not been collected in a systematic manner with spatial and temporal comparisons to assess the biogeochemical cycles within the Red Sea comprehensively. However, the compiled data can be used to better characterize the biogeochemical cycles of the Red Sea as other researchers add new data. The reported datasets represent the first measured in the Red Sea wherein the fractions of organic matter, including biopolymers, humic substances, building blocks, LMW neutrals, and LMW acids (very expensive to measure), are linked with measurements of algae, bacteria, TOC, and TEP.

2. Material and methods

2.1. Compilation and comparison of available data

There have been several investigations on organic matter, including TEP, collected at depths near the sea surface along the Red Sea coast of Saudi Arabia, with the main focus to establish the relationships between seawater organic matter content and the potential for membrane biofouling in seawater desalination facilities [9–18] (Fig. 1, blue dot locations). These shallow nearshore data were compiled and assessed to compare to the newly collected offshore data and to assess statistical relationships between various organic parameters. Note that these data have been collected at many different times of the year and were not used to attempt the characterization of the natural seasonal variations and the overall biochemical activity in the nearshore area of the Red Sea.

2.2. Seawater vertical profiles in the Red Sea

Seawater properties of the water column were measured at four sites (A–D) north of Jeddah, along the Saudi

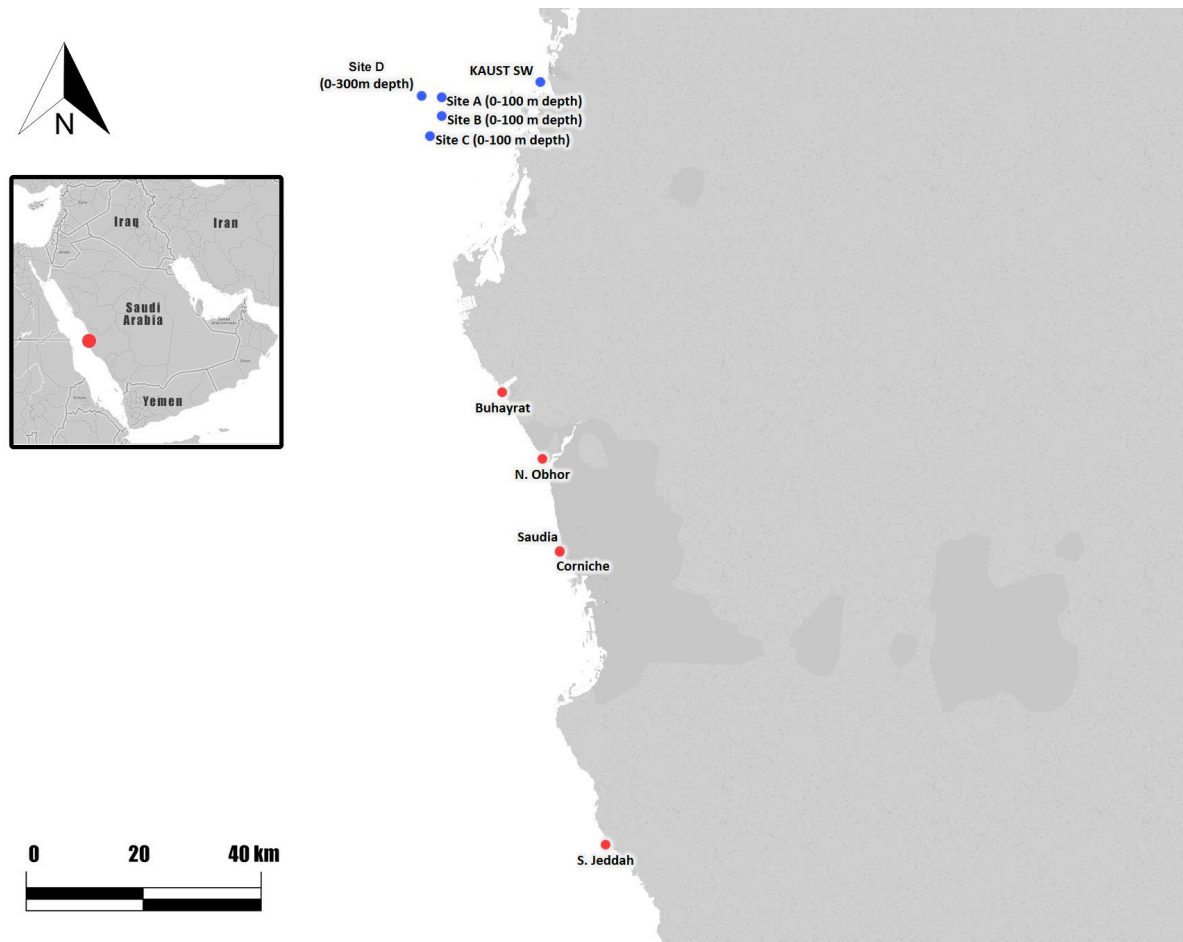


Fig. 1. Map showing the sampling profile locations in the Red Sea.

Arabian coast of the Red Sea in deep water areas (>1,000 m) (Fig. 1). *In situ* vertical profiles of temperature, salinity, dissolved oxygen (DO), pH, turbidity, chlorophyll-a (fluorescence), and photosynthetically active radiation (PAR) were determined with a multi-sensor assembly fitted to a Rosette carousel holding a set of Niskin water sampling bottles (General Oceanics, USA). Continuous vertical profiling was conducted from sea surface to 90 m depth at sites A–C, with seawater samples obtained at 10 m depth intervals for the analysis of organic parameters. At site D, continuous vertical profiles of physicochemical parameters were taken from 7 m below sea surface to 300 m depth, with seawater samples collected for measurement of organic parameters obtained at 10 m intervals from the surface to 100 m depth and at 20 m intervals thereafter to 300 m depth. Sampling at sites A–C was conducted in April 2014, whereas at site D in February 2015. The sample timing was based on ship availability and the data collected cannot be used to fully characterize the Red Sea in deep water located far from the coast. Note that the water depth drops almost vertically to greater than 1,000 m beginning in the nearshore at the 20 m contour [11].

The multi-sensor assembly included the Sea-Bird 911 plus CTD for salinity, temperature and depth profiling, with a DO add-on sensor; Wet Labs ECO AFL/FL (Sea-Bird Scientific) was used for turbidity and fluorescence detection;

and a biospherical light sensor (LI-COR) was used for PAR measurement. All sensors were pre-calibrated according to manufacturer specifications before actual use in field sampling and was normalized.

2.3. Quantification and characterization of microalgae and bacteria

Microalgal abundances in water samples were determined by flow cytometry, using a BD FACSVerser flow cytometer for counting and characterizing algal cells, as described by van der Merwe et al. [46]. An Accuri flow cytometer was used to measure bacterial abundance. Flow cytometry enables a rapid and accurate counting of microorganisms [47]. Lasers were used to excite both unstained autofluorescent organisms (algae) and stained bacterial cells with the red laser wavelength set at 640 nm and the blue laser at 488 nm. Algal cell counting was performed by combining 500 μL of each sample with a 1 μL volume of a standard containing 1 μm beads to calibrate size in a 10 mL tube. The tube was then vortexed and measured at high flow rate with a 200 μL injection volume for 2 min. The counting procedure was repeated three times to assess the precision of measurements. The different types of algae, *Prochlorococcus*, pico/nanoplankton and cyanobacteria,

were distinguished based on their autofluorescence as well as by the cell side-angle scatter, which was used to identify them by size [48].

A comparative protocol employing SYBR®Green stain was used for bacteria counting. A volume of 500 μL from each sample was transferred to a 10 mL tube, incubated in 35°C water bath for 10 min. SYBR® Green dye was added at a 5 μL into a 500 μL aliquot to stain the cells. The sample was vortexed and incubated for 10 min. The prepared samples were then analyzed at a medium flow setting with a 50 μL injection volume for 1 min. For validation, eight-peak calibration beads were used. Triplicate measurements were made on each sample to assess measurement precision.

2.4. Measurement of TOC and NOM fractions

TOC concentration was measured with a Shimadzu TOC-VCSH (Tokyo, Japan). Fractions of DOC, including biopolymers, humic substances, building blocks, LMW neutrals, and LMW acids, were determined by liquid chromatography organic carbon detector (LCOCD, DOC-Labor), using a size exclusion chromatography column Toyopearl HW-50S (TOSOH, Tokyo, Japan), following the methods described by Huber et al. [49]. A calibration curve was established for both molecular masses of humic substances and detector sensitivity before sample measurements. Humic acid and fulvic acid standards (Suwannee River Standard II) were used for the molecular mass calibration, whereas potassium hydrogen phthalate and potassium nitrate (KNO_3) were used for sensitivity calibration based on Huber et al. [49].

All seawater samples for LCOCD were manually pre-filtered using a 0.45 μm syringe filter to exclude the undissolved particulate organics. Before sample analysis, a system cleaning was performed by injection of 4,000 μL of 0.1 mol/L NaOH through the column for 260 min. After cleaning, 2,000 μL of the sample was injected for analysis at 180 min retention time and 1.5 mL/min flow rate. A mobile phase of phosphate buffer, with 28 mmol STD and 6.58 pH, was used to carry the sample through the system. The resulting chromatogram showed a plot of signal response of different organic fractions against retention time. Manual integration of the data, also following Huber et al. [49], was performed to determine the concentrations of the different organic fractions, including biopolymers, humic substances, building blocks, LMW acids and LMW neutrals.

2.5. TEP measurement

Both p-TEP and c-TEP were simultaneously determined in each collected sample. TEP analysis was based on the method developed by Passow and Alldredge [50], which involves sample filtration, membrane staining with Alcian blue, and then UV spectrometry. A staining solution was prepared from 0.06% (m/v) Alcian blue 8GX (Fluka) in acetate buffer solution (pH 4) and freshly pre-filtered through a 0.2 μm polycarbonate filter before usage. A 300 mL volume of seawater from each water sample was filtered through a 0.4 μm pore size polycarbonate membrane using an adjustable vacuum pump at low constant vacuum. After filtration, the membrane was rinsed with 10 mL of Milli-Q water to prevent the Alcian blue from coagulating, as salts may

remain on the filter after seawater filtration, thus avoiding the likelihood of overestimating the TEP concentration. The retained TEP particles on the membrane surface were then stained with the Alcian blue dye for 10 s. After staining, the membrane was flushed with 10 mL of Milli-Q water to remove any excess dye. The flushed membrane was then placed into a small beaker, where it was soaked in 80% sulfuric acid for 6 h to extract the dye that was bound to the p-TEP. Finally, the absorbance of the acid solution was measured by a UV spectrometer at 752 nm wavelength to determine the TEP concentration. The same methodology was applied to determine the colloidal TEP, except that a 250 mL volume of water sample from 0.4 μm polycarbonate membrane permeate was filtered through a 0.1 μm pore size to allow deposition of the c-TEP on the membrane surface.

To relate the measured UV absorbance values to TEP concentrations, a calibration curve was established. Xanthan gum solutions with different volumes (0, 0.5, 1, 2, 3 mL) were used to obtain the calibration curve (Fig. 2). Note that the calibration curve for samples collected at sites A, B, and C are shown in Fig. 2a and the curve for site D is shown as Fig. 2b. The TOC concentrations of xanthan gum before and after 0.4 μm filtration were analyzed, and the TOC concentration difference was used to calculate the gum mass on each filter and the TEP concentration was estimated using the calibration curve. The same procedures were used for the 0.1 μm membrane to establish the calibration curve for colloidal particles. Afterwards, the TEP concentration was expressed in terms of Xanthan Gum equivalent in $\mu\text{g Xeq/L}$ by dividing the TEP mass by the corresponding volume of TEP samples. Because particulate and colloidal TEP are determined indirectly, these values must be considered to be semi-quantitative. The new method developed by Villacorte et al. [6] for TEP measurement was not used, as it would limit the comparability of the measured data with previous results.

2.6. Statistical methods used for data comparison

It is essential to perform a multidimensional regression analysis at a certain meaningful abstraction level to find interesting patterns and to determine whether the results in a data set are statistically significant [51]. Multiple regression has been used by several researchers and practitioners for theory testing or explanation purposes. The question of interest becomes understanding the significance of the variables, and the variation and interaction between them [52]. It is herein desired to highlight the correlation between TEP concentrations and abundance of microalgae, bacteria, TOC, and dissolved fractions of NOM, including biopolymers. Thus, a multi-dimensional regression analysis, a correlation matrix, and two-way analysis of variance (ANOVA) with replication were performed to test the interaction and statistical significance between the various organic properties. In order to perform multiple regression analysis, there must be a relationship between the outcome variable and the independent variables to assess whether the residuals are normally distributed, and the independent variables should not be highly correlated with each other [53,54]. The interdependency was tested using Pearson's bivariate correlations matrix. The spatial/temporal variation of the data is not

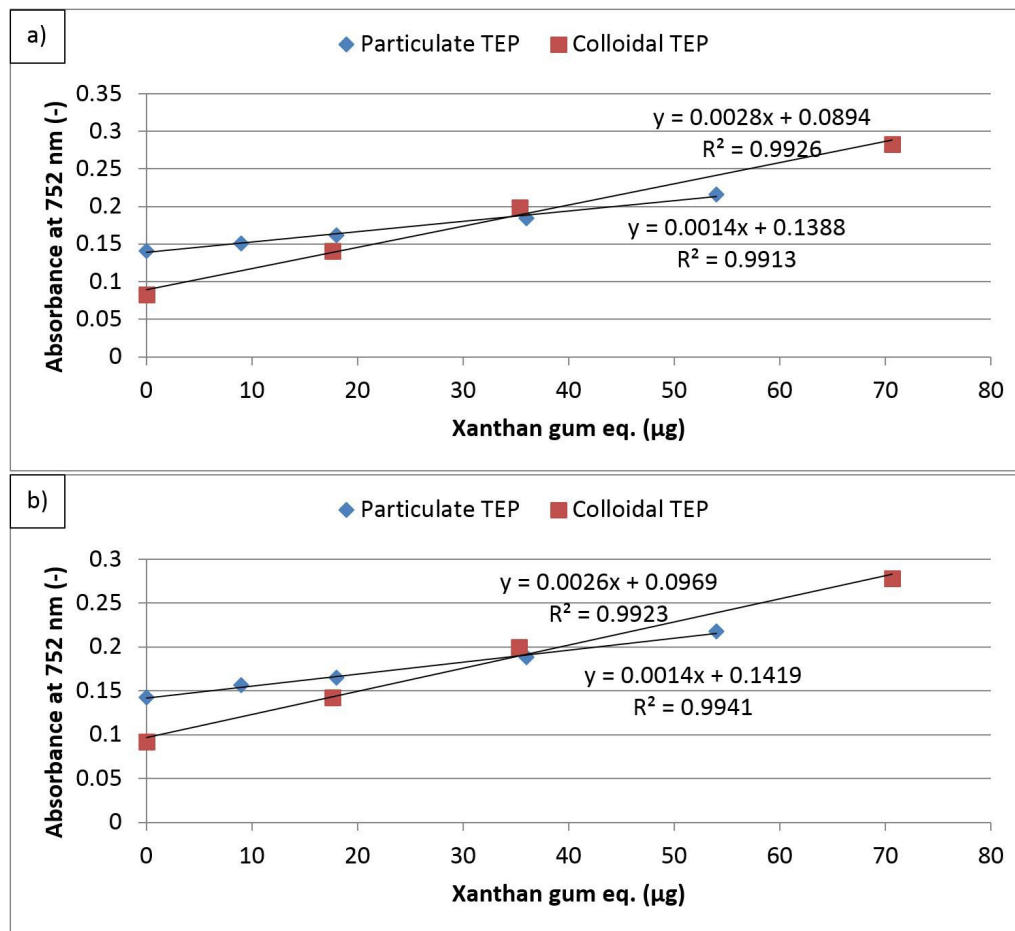


Fig. 2. Xanthan gum standard calibration curves for determination of p-TEP and c-TEP. Curve (a) is for sites A, B, and C and curve (b) is for site D.

the focus of this paper and the intricacies of dominance or relative weight between variables were not considered.

The correlation coefficients, R^2 and p -values, were calculated to assess the relationship, statistical significance and interaction between various organic properties. The correlation matrix is an identity matrix, which would indicate that variables are related or unrelated. Multi regression analysis is used to understand the significance of the two or more organic properties in predicting the value of a criterion variables (TEP and biopolymers). The two-way ANOVA analyses were used to determine the significant difference and interaction among the sites and organic properties. When the p -value was below 0.05, the null hypothesis was void and the relationship was deemed to be significant.

3. Results

3.1. Variations in salinity, temperature, fluorescence, pH, dissolved oxygen, PAR/irradiance, biospherical/loric, and turbidity

The thermocline in the three profiles (sites A–C) collected to a 90 m depth showed a slight decrease in temperature from near 29°C to between 24°C and 25°C at 90 m below surface (Fig. 3). The decline in temperature was

relatively gradual at all three sites. In the deep profile (site D), the temperature declined from about 26.5°C at the surface to about 22°C at 300 m. An inflection point occurred at about 115 m and the change in temperature below this depth to 300 m was only about 2.5°C (Fig. 4). The difference in the temperature at the sea surface between profiles was likely caused by the time of year of measurements, with the 90 m profiles occurring in April vs. the 300 m profile in February which is the peak of winter in the study area.

The halocline showed similar salinity variations in the 90 m profiles with a slight, rather uniform increase from about 39 ppt at surface to 40 ppt at 90 m (Fig. 3). A slightly lower salinity gradient coinciding with a slightly higher temperature gradient occurred at site B. The salinity change in the 300 m profile showed a similar pattern from about 39–40 ppt in the upper 115 m, but an inflection occurred at about 115 m wherein the rate of increase declined to a tenth of a ppt over the lower 185 m. The inflection point showing a slope change for both temperature and salinity occurred at about the same depth which may indicate the presence of two water masses (Figs. 3 and 4).

The vertical trends in pH also exhibited minimal variations down to 90 m at sites A–C (Fig. 3), but with slightly lower pH values at site A (7.9–8.0) than at sites B and C

(8.0–8.1). In the deep profile (site D), pH was nearly stable at about 8.3 until 115 m, and then steadily decreased to 8.1 at 300 m (Fig. 4).

Dissolved oxygen (DO) concentrations in the shallow profiles at all three sites showed high variability (6–12.5 mg/L) in the top layer (unknown reason for variation), but with relative stability at about 5 mg/L from 20 to 90 m (Fig. 3). DO in the deep profile was at lower concentrations (0.8–1.5 mg/L) near the surface, increasing to around 2 mg/L at 115 m and then steadily declined to about 0.6 mg/L at 300 m with a saturation of only 10%.

The vertical pattern in chlorophyll *a* (chl-*a*) concentrations markedly differed between shallow and deep profiles (Figs. 3 and 4). At sites A–C, chl-*a* was slightly detected at the surface but abruptly increased from 0.3 to

1.2 mg/m³ within 50–75 m and thereafter declined to near 0.2 mg/m³ at sites A, B, and C. Chl-*a* concentrations were relatively low in the deep profile, decreasing from about 0.45 mg/m³ at the surface to about 0.06 mg/m³ at 100 m, from which it remained unchanged until 300 m. Note that these chl-*a* concentrations were based on *in situ* fluorescence detection using a sensor that was pre-calibrated with a chlorophyll standard from the manufacturer (Wet Labs). As chlorophyll fluorescence may vary with cell physiological condition, time of day, light regime, and other factors, and since the sensor was not field-validated after calibration, the present chl-*a* values should thus be considered semi-quantitative.

PAR levels at sites B and C were initially recorded at 600–700 μmol/m²/s at the surface and then steeply decreased to 130–180 μmol/m²/s at 20 m depth, from where it further

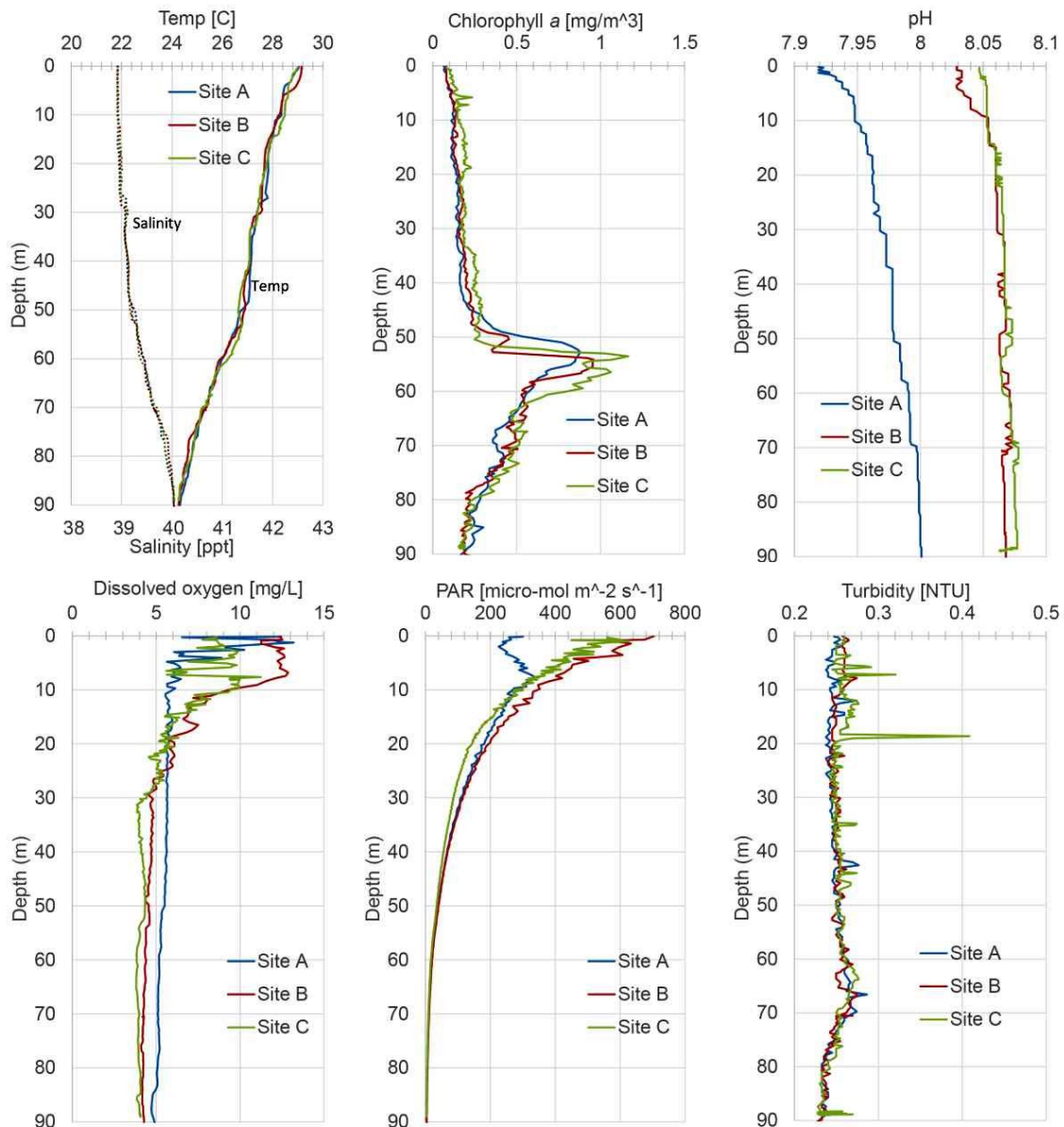


Fig. 3. Physical data from the three 90 m profile.

decreased gradually until 90 m depth (Fig. 3). At site A, where the measurement was done at an earlier time, PAR varied between 220 and 300 $\mu\text{mol}/\text{m}^2/\text{s}$ within the top 10 m layer and then coincided with the same values at sites B and C. PAR in the deep profile (site D) steeply declined from about 240 $\mu\text{mol}/\text{m}^2/\text{s}$ near the surface to about 20 $\mu\text{mol}/\text{m}^2/\text{s}$ at 40 m depth, after which it gradually decreased to near zero at about 75 m, which is generally similar to the trend in the shallow profiles (Figs. 3 and 4). The depths at which the PAR levels were at 1% of the surface values were in range of 38–54 m for all sites.

Turbidity was generally low in the vertical profiles at all sites. Turbidity varied in the narrow range of 0.2–0.3 NTU, with only a few spikes up to 0.4 NTU, in all three shallow profiles (Fig. 3). In the deep profile (site D), most turbidity values were within 0.1–0.15 NTU, with intermittent spikes up to 0.2 NTU below 75 m depth (Fig. 4).

3.2. Algae and cyanobacteria concentrations

Total concentrations of algae and cyanobacteria (summed) with depth at the shallow and deep sampling stations are shown in Figs. 5 and 6, respectively. Previous results on total algal and cyanobacterial abundances, all collected from surface layers close to shore in the same study area, are compiled in Table 1, with a range of 1,677–137,363 cells/mL (mean 44,383 cells/mL out of 38 samples). Total algal and cyanobacterial concentrations from the surface at the shallow stations (A–C) during the present study were comparable to the mean of the previous data, while the surface concentration at the deep station (D) was close to the reported maximum (Figs. 5 and 6, Table 1).

The vertical profiles of algal and cyanobacteria concentrations by group (cyanobacteria, *Prochlorococcus* and pico/nanoplankton) are shown in Figs. 5 and 6 for the

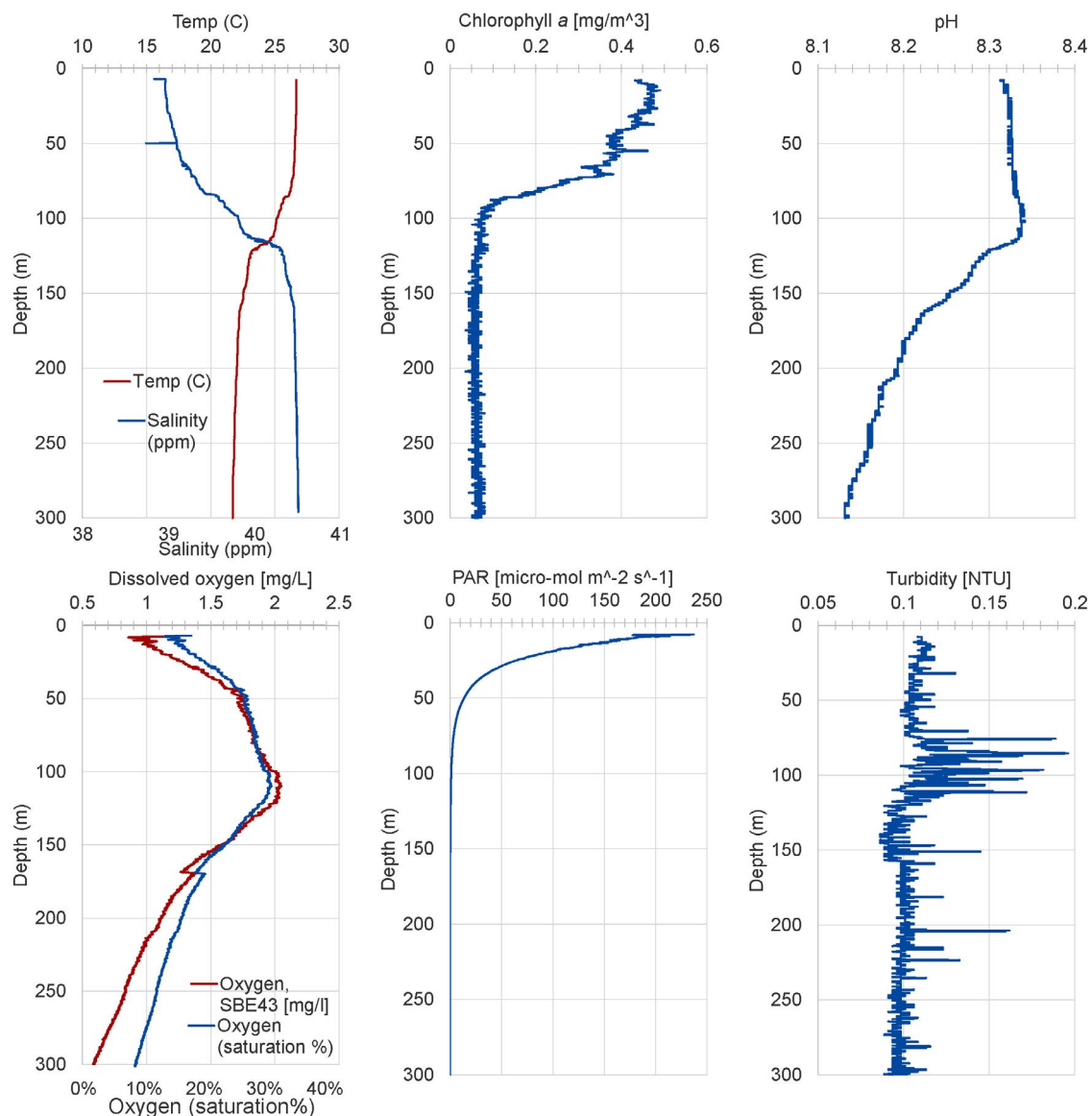


Fig. 4. Physical data from the 300 m profile.

shallow (A–C) and deep (D) sites, respectively. At sites A–C, cyanobacteria were more abundant near the surface (top 10 m layer), below that *Prochlorococcus* was more predominant, with peak concentrations at about 50 m (Fig. 5). In general, algal and cyanobacterial concentrations showed a substantial decline below 80 m at all sites. The same compositional and abundance trends were exhibited in the deep profile, except that cyanobacteria had higher concentrations near the surface in the deep profile while *Prochlorococcus* was relatively denser at subsurface depths in the shallow profiles (Fig. 6). In addition, the concentrations of pico/nanoplankton in the upper layers were relatively higher at the deep (D) site compared to the shallow sites (A–C) (Figs. 5 and 6).

3.3. Bacteria concentrations

The vertical trends in bacterial concentrations during the present study are shown in Figs. 7 and 8, indicating

higher cell densities in the upper 50 m layer at the deep site D compared to sites A–C. Previous results on nearshore bacterial concentrations from the same study area ranged from 1.13×10^5 to 2.18×10^6 cells m/L (mean 5.26×10^5 cells m/L; 40 samples; Table 1). The new data on offshore surface concentrations of bacteria are comparable to the average of the nearshore results (Table 1, Figs. 7 and 8). Bacterial abundance generally declined with depth, with a decrement of about 4.00×10^5 to 9.00×10^4 cells m/L from the surface to 90 m depth at sites A–C (Fig. 7) and from about 5.00×10^5 cells m/L at the surface to 1.60×10^5 cells m/L at 160 m and to 1.00×10^5 cells m/L at 300 m at site D (Fig. 8).

3.4. Total organic carbon

TOC concentrations exhibited only minor differences between the sites, with fluctuations within a narrow range in the upper 50 m layer at both the shallow and deep sites

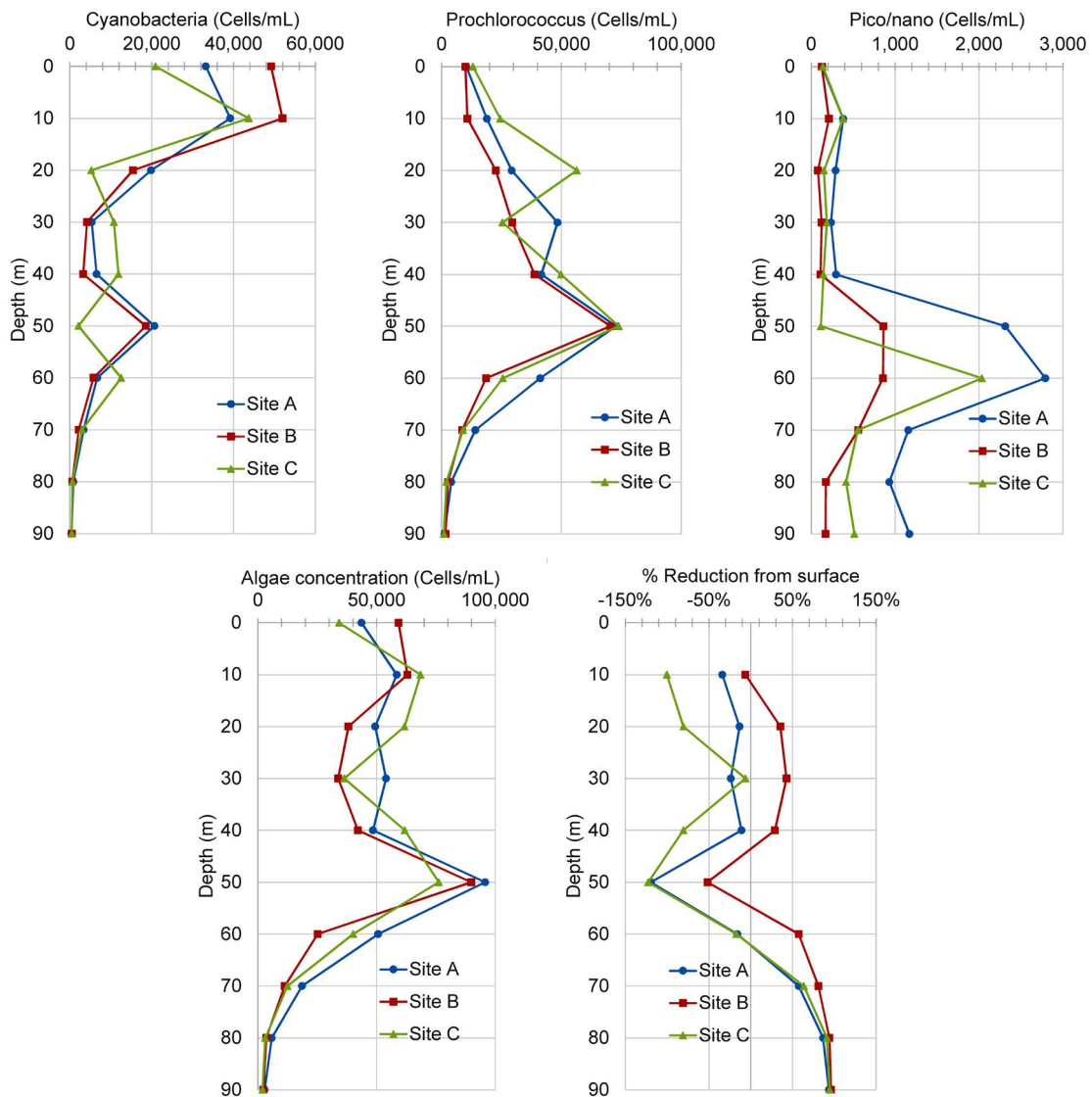


Fig. 5. Algal and cyanobacteria composition and concentration data from the three 90 m profiles.

Table 1
Compilation of related nearshore data from previous studies [9–18]

Location	Date	Depth (m)	Total algae and cyanobacteria (cells/mL)	Bacteria (cells/mL)	TOC (mg/L)	NOM ($\mu\text{g/L}$)				TEP $\mu\text{g Xeq/L}$		
						Biopolymers	Humic substances	Building Blocks	LMWN	LWMA	p-TEP	c-TEP
N. Obhor	1/8/2014	Surface	30,524	112,790	0.89	76	345	103	168	88	162	-
Corniche	1/11/2014	Surface	3,603	196,377	0.94	90	360	91	192	94	121	73
S. Jeddah	1/9/2014	Surface	1,677	264,728	1.02	116	351	139	197	103	157	122
Buhayrat	-	Surface	30,395	320,870	1.053	47	343	82	16	85	58	-
Site A (Buhayrat)	1/7/2014	Surface	14,956	179,837	0.88	63	367	131	230	130	123	130
Site B (Saudia)	5/25/2013	Surface	23,773	317,174	0.83	84	289	101	45	101	53	56
N. Obhor	10/25/2014	Surface	129,738	520,350	1.1	57	205	95	163	18	318	90
Corniche	11/6/2014	Surface	89,033	254,450	1.0	44	201	86	249	16	249	120
S. Jeddah	12/24/2014	Surface	42,923	216,400	0.9	32	196	95	276	24	255	115
N. Obhor	6/7/2015	Surface	-	707,100	1.262	40	194	85	466	19	111	223
N. Obhor	6/17/2015	Surface	-	-	1.034	42	185	99	231	18	-	-
N. Obhor	7/1/2015	Surface	108,740	282,450	1.162	49	192	105	313	21	142	189
N. Obhor	7/12/2015	Surface	87,615	252,233	1.036	50	188	105	477	31	-	-
N. Obhor	8/3/2015	Surface	135,603	908,100	1.104	80	209	122	269	31	231	216
N. Obhor	8/16/2015	Surface	49,770	1,764,850	1.118	71	184	111	284	16	-	-
Saudia	6/7/2015	Surface	-	317,567	1.055	29	172	100	369	21	215	242
Saudia	6/17/2015	Surface	-	-	1.233	46	189	84	183	14	-	-
Saudia	7/1/2015	Surface	61,925	583,400	1.287	44	190	93	152	14	146	213
Saudia	7/12/2015	Surface	137,363	1,070,400	1.294	40	159	82	188	16	-	-
Saudia	8/3/2015	Surface	53,810	1,736,450	1.164	93	180	111	238	19	347	287
Saudia	8/16/2015	Surface	43,060	2,182,550	1.181	83	208	103	276	15	-	-
N. Obhor	2015/4/2	Surface	91,870	1,356,600	1.10	55	214	98	387	14	261	132
KAUST SW	5/3/2014	Surface	4,766	273,400	1.42	29	217	119	315	24	278	100
KAUST SW	5/22/2014	Surface	9,350	236,000	1.037	55	197	121	252	17	346	97
KAUST SW	6/11/2014	Surface	3,140	287,850	0.992	36	246	81	319	18	229	170
KAUST SW	7/3/2014	Surface	4,958	324,600	1.085	43	212	151	227	10	85	127
*KAUST SW	7/19/2014	Surface	11,080	389,450	0.97	53	212	91	233	16	99	117

(continued)

Table 1 continued

Location	Date	Depth (m)	Total algae and cyanobacteria (cells/mL)	Bacteria (cells/mL)	TOC (mg/L)	NOM (µg/L)				TEP µg Xeq/L		
						Humic substances	Biopolymers	Building Blocks	LMWN	LWMA	p-TEP	c-TEP
⁶ KAUST SW	8/18/2014	Surface	6,057	316,450	1.112	201	40	88	225	14	82	112
⁶ KAUST SW	9/18/2014	Surface	52,453	321,250	0.923	193	35	93	171	13	97	69
⁶ KAUST SW	10/21/2014	Surface	12,228	630,600	0.831	193	39	108	256	16	213	50
⁶ KAUST SW	12/3/2-14	Surface	10,673	347,133	1.004	189	33	101	288	23	138	43
⁶ KAUST SW	2/11/2015	Surface	12,890	292,500	1.275	200	36	102	343	31	182	87
⁶ KAUST SW	5/21/2015	Surface	28,009	450,800	0.93	177	31	93	236	25	143	50
⁶ KAUST SW	8/6/2015	Surface	44,153	336,900	1.041	184	42	86	229	18	186	36
⁶ KAUST SW	9/17/2015	Surface	52,453	297,867	1.084	188	28	86	230	24	300	105
⁷ KAUST SW	9/30/2016	Surface	11,955	369,300	1.073	429	112	213	385	86	-	-
⁷ KAUST SW	10/2/2014	Surface	10,600	367,000	0.993	363	105	193	353	92	307	-
⁷ KAUST SW	10/9/2014	Surface	17,777	368,463	0.944	373	140	218	335	79	333	-
⁷ KAUST SW	10/16/2014	Surface	22,030	319,950	0.961	340	88	216	346	80	206	-
⁷ KAUST SW	10/27/2014	Surface	42,550	297,700	0.917	348	164	260	468	49	318	-
⁷ KAUST SW	11/6/2014	Surface	86,033	587,200	0.864	442	73	93	470	73	124	-
⁷ KAUST SW	11/17/2014	Surface	107,030	673,700	0.897	374	71	221	352	81	83	-
No. of samples			38	40	42	42	42	42	42	42	35	27
Range in values			1,677–137,363	112,790–2,182,550	0.830–1.420	159–442	28–164	81–260	16–477	10–130	53–347	36–287
Average			44,383	525,820	1	248	62	118	271	40	191	125

¹Rachman et al. [13]; ²Dehwah et al. [9]; ³Dehwah and Missimer [10]; ⁴Alshahri et al. [15]; ⁵Dehwah et al. [16]; ⁶Dehwah and Missimer [17]; ⁷Dehwah and Missimer [18].

(Figs. 7 and 8). Nearshore data on TOC ranged from 0.83 to 1.42 mg/L, with an average of 1.0 mg/L from 42 measurements (Table 1). In the offshore near-surface profiles, the TOC ranged from 0.99 to 1.35 mg/L.

TOC generally declined with depth at all sites, although only within a narrow range at sites A–C between 1.2 mg/L at surface and 0.9 mg/L at 90 m depth. The decline in the deeper profile (D) was from 1.1 mg/L at surface to 1.0 mg/L at 120 m and then to 0.75 mg/L at 300 m.

3.5. Particulate and colloidal TEP concentrations

Nearshore p-TEP and c-TEP showed considerable variation in concentrations with ranges of 53–347 (mean 191) and 36–287 (125) $\mu\text{g Xeq/L}$, respectively (Table 1). Comparable ranges of concentration for both parameters were found offshore, except for the markedly higher c-TEP concentrations in the vertical profile at site A (Figs. 7 and 8).

Both p-TEP and c-TEP generally declined with depth, although with fluctuations between 50 and 100 m depth and an elevated value at 200 m depth in the deep profile (D). The difference in concentrations was more pronounced for c-TEP in the deep profile, from 265 $\mu\text{g Xeq/L}$ at 10 m to about 60 $\mu\text{g Xeq/L}$ at 300 m. The change in concentration of p-TEP with depth in the deep profile was relatively slight, from about 285 $\mu\text{g Xeq/L}$ at 40 m to 170 $\mu\text{g Xeq/L}$ at 300 m. At the shallow sites, both p-TEP and c-TEP trends with depth showed similar patterns between sites B and C, except that c-TEP was unusually low in the surface layer at site C (Fig. 7).

3.6. NOM fractions

There was considerable variability in concentrations of the NOM fractions in nearshore seawater (Table 1). The range in concentration, number of samples, and average of the

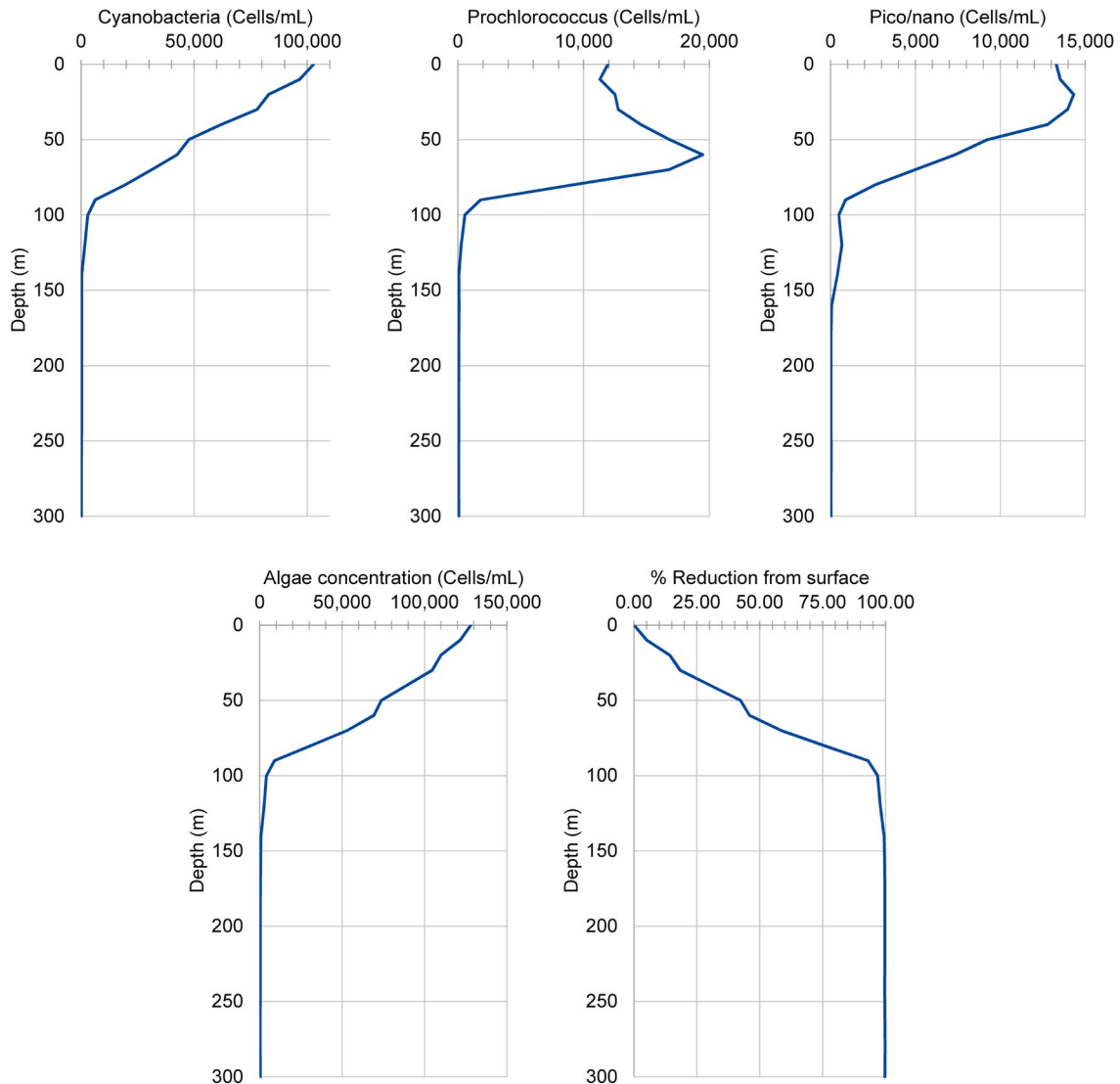


Fig. 6. Algal and cyanobacteria composition and concentration data from the 300 m profile.

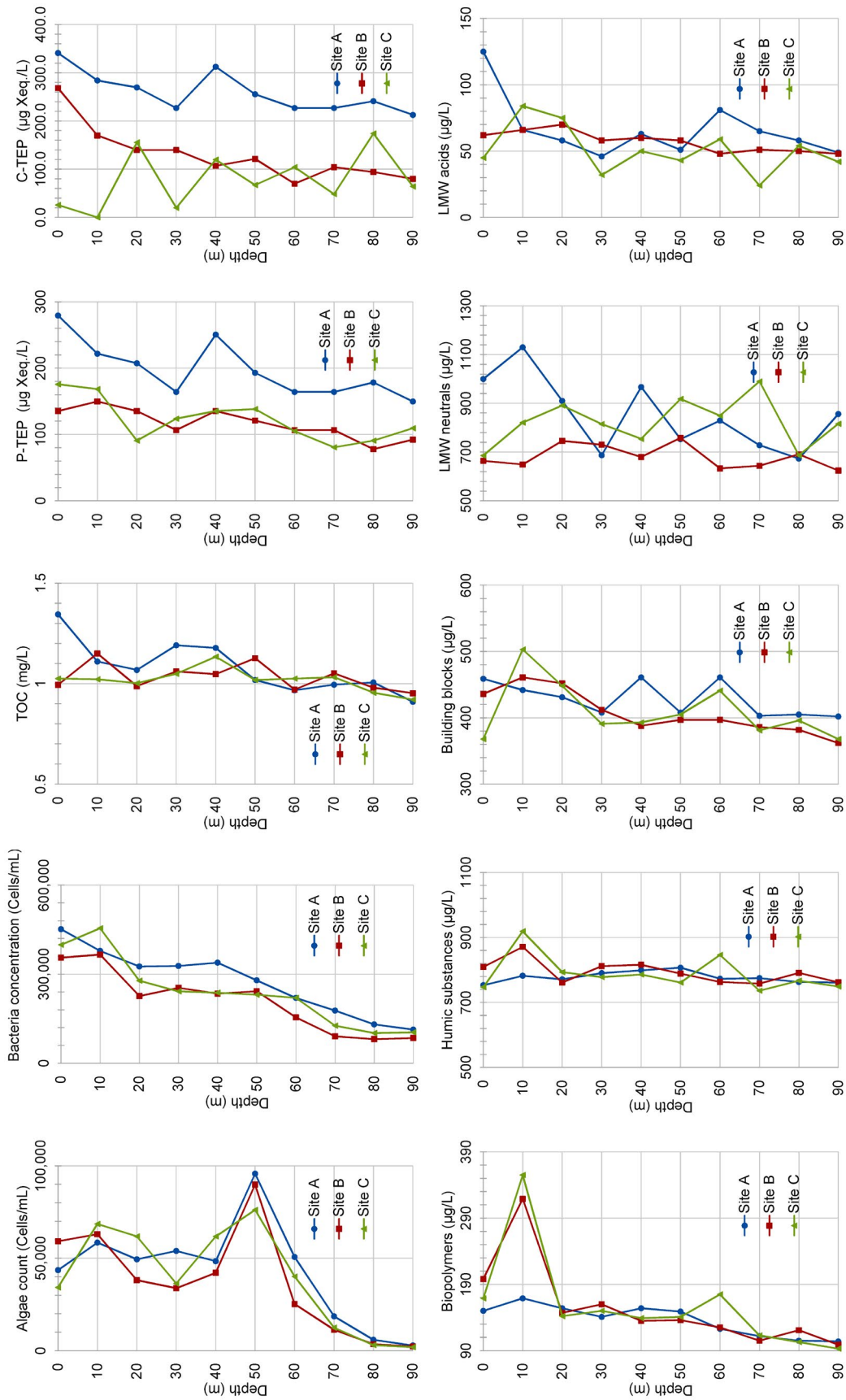


Fig. 7. Organic carbon concentrations for the three 90 m profiles.

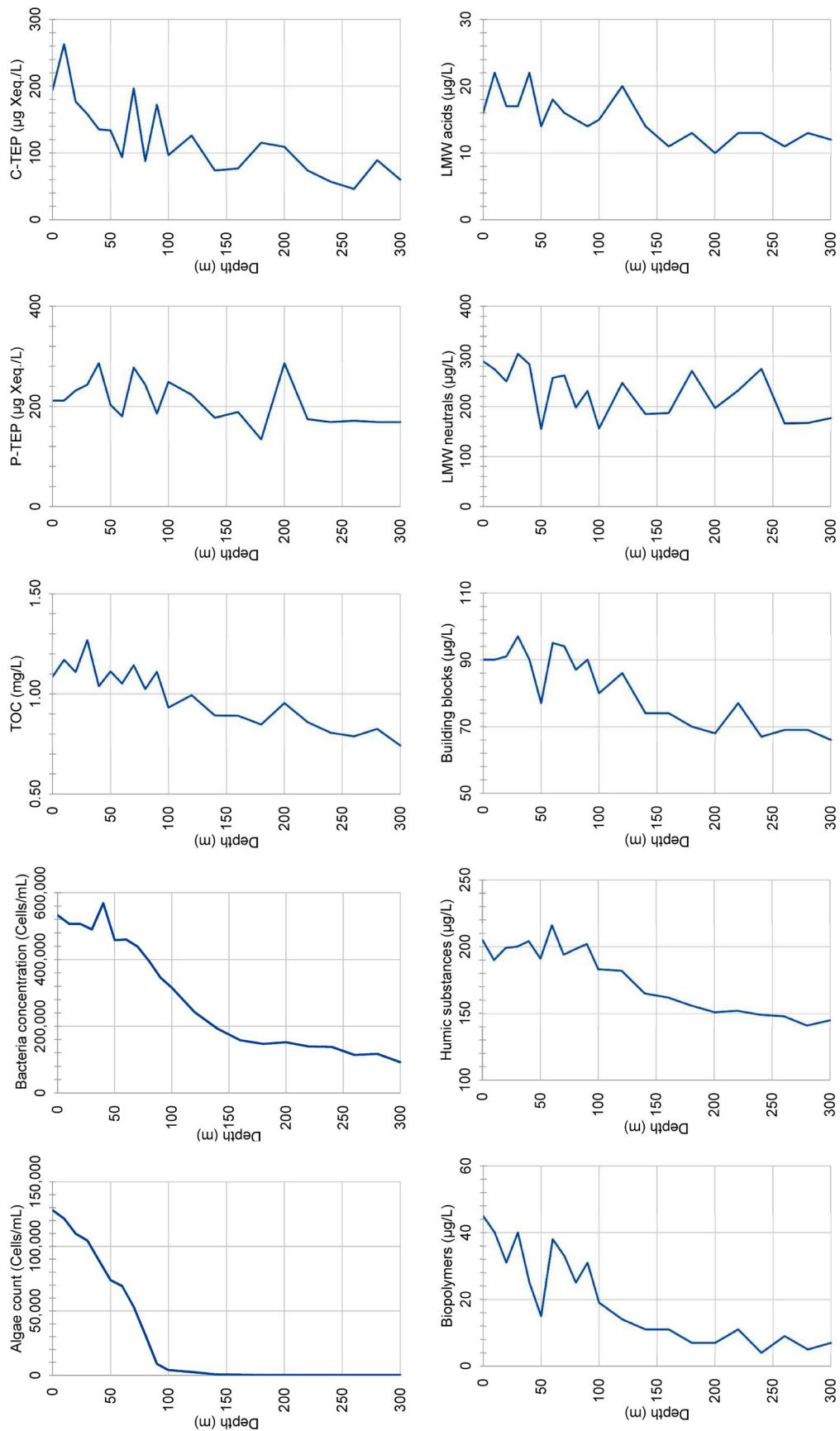


Fig. 8. Organic carbon concentrations from the 300 m profile.

concentrations are the following: biopolymers (28–164 µg/L, 42, 62 µg/L), humic substances (159–442 µg/L, 42, 248 µg/L), building blocks (81–260 µg/L, 42, 118 µg/L), LMW neutrals (16–477 µg/L, 42, 271 µg/L), and LMW acids (10–130 µg/L, 42, 40 µg/L). The range in biopolymer concentrations in the surface offshore samples are similar to the nearshore samples. All of the NOM fractions have higher concentrations at the sites A, B, and C profiles compared to the deep profile (D).

The biopolymer fraction of NOM shows a general reduction with depth in all offshore profiles. At sites A, B, and C there is a spike in biopolymers at 10 m with minor variation between 10 to 90 m. In the deeper profile, there is considerable variation in the photic zone with the surface having the highest value and subsequent spikes occurring at 30 and 60 m. There is a constant downward trend in concentration beginning at about 90 m.

Humic substances concentrations showed only minor variations with depth in the shallow profiles, but the deep profile showed a reduction by about 29% from 90 to 300 m depth. There is a general decreasing trend in concentration of building blocks with depth at the deep site and only minimal differences throughout the depth profiles at sites A–C (Figs. 7 and 8). The concentrations of LMW neutrals at the shallow sites were the highest amongst NOM fractions, although with a wide range of variation. In contrast, LMW acids had the lowest concentrations without marked discrepancies in concentration in the vertical profiles between sites A and C, but a general reduction occurred below 120 m in the deep profile (Figs. 7 and 8).

4. Discussion

4.1. Algal and cyanobacterial concentrations

The flow cytometry approach was used in this study in characterizing and enumerating the small size classes of phytoplankton and cyanobacteria that are readily distinguishable on the basis of cell size and autofluorescence. Thus, cyanobacteria (presumably *Synechococcus* spp.), *Prochlorococcus*, and the general class of pico/nanoplankton were numerically dominant, with very few larger eukaryotic algal species detected. This is consistent with prior studies that reported that phytoplankton in the oligotrophic northern Red Sea and Gulf of Aqaba are dominated (>95%) by cells <5 µm in size [55,56]. Only during the summer does the large macroalgae *Trichodesmium* sp., also become prominent. As reported here, algae ranging from five to several hundred µm are extremely scarce, although not totally absent [57,58].

4.2. Statistical significance and dependency of p-TEP, c-TEP, and biopolymers

The two-way ANOVA was employed to provide an important insight into the pattern of the data and its interdependency. Each organic parameter (sample) has been drawn independently of the other parameters and is normally distributed. The analysis shows that there is a significant difference ($p < 0.05$) in the mean of the concentrations of TEP, bacteria, algae, TOC, and biopolymer, and the mean of the sites. Also, it shows that there is no interdependency between the sites where samples are measured (Table 2).

Table 2
Two-way ANOVA p -value for interdependency of site and its attributes

Source of variation	p -value
Sample (offshore and nearshore site)	0.00702
Attributes (bacteria, algae, TOC, biopolymer and TEP)	0.00000
Interaction	0.00011

In order to validate the appropriateness of the multiple regression analysis, multicollinearity of the concentration of bacteria, algae, biopolymer, TOC, p-TEP, and c-TEP were checked using a bivariate correlation matrix (Table 3). The matrix of Pearson's bivariate correlations among all independent variables shows that the magnitude of the correlation coefficients are less than 0.8.

A series of multi regression statistical analyses were performed to test if there are significant relationships between dependent and independent variables/organic properties. A summary of results of this analysis is presented and shown in Table 3.

4.3. Particulate transparent exopolymer particles

Multiple regression analysis between the p-TEP and the concentrations of bacteria, and algae, shows a significant statistical correlation for all offshore profiles while the concentration of TOC is not significant parameter for the p-TEP. The overall regression is significant when the three variables are considered as a group. The individual variables and their significance are shown in Tables 3 and 4. However, the analysis shows that there was no statistically-significant relationship between p-TEP and the three parameters in the shallow, nearshore samples (Tables 3 and 4).

4.4. Colloidal transparent exopolymer particles

The overall regression between the c-TEP and the concentrations of bacteria, algae, and TOC shows no significant statistical correlation for the shallow profiles (sites A, B, C) and deep (Site D) profile. However, the individual linear regression analysis shows statistically-significant relationships between c-TEP and TOC, and c-TEP and bacteria. There is no statistical relationship of significance between p-TEP and c-TEP with an adjusted $R^2 = 0.12$. Also, the nearshore samples show that there was no statistically-significant relationship between c-TEP and TOC and bacteria (Tables 3 and 4).

4.5. Biopolymers

Multiple regression analysis between the biopolymers and the concentrations of bacteria, p-TEP and c-TEP shows a significant statistical correlation for all the offshore profiles while the concentration of algal and cyanobacteria is not a significant predictor of the biopolymers. The overall regression is significant when the four variables are considered as a group. The individual variables and their significance are

shown in Table 3. The relationship between the biopolymers and all the four independent variables shows no significant statistical correlation in the shallow, nearshore samples.

4.6. Correlations between TEP, bacteria, algae, the biopolymer fraction of NOM, and TOC

TEP is composed of acidic polysaccharides and some large proteins that occur mostly in the biopolymer fraction of NOM and some of the proteins within the humic substances part of NOM [4,8]. TEP can be produced both abiotically and as extracellular discharges from bacteria and algae [21,22,30,38,59]. Therefore, there should be some statistical relationship between TEP, the biopolymer fraction of NOM, bacterial concentration or algae concentration.

A series of statistical analyses were performed to test if there are significant relationships between the various organic properties (Tables 2–4). There is a significant statistical relationship between p-TEP with algae (grouped with cyanobacteria) and bacteria but this does not occur with c-TEP. There is a significant statistical relationship between the biopolymer fraction of NOM with bacteria, p-TEP, and c-TEP in all of the offshore profiles. Since c-TEP is considered to be the precursor to formation of p-TEP, the association with biopolymers is logical and could indicate potential for abiotic assembly in the water column.

The relationship between the biopolymers and bacterial concentrations shows a significant statistical correlation in all offshore profiles. These relationships suggest that extracellular discharges of polysaccharides and proteins from the bacteria and algae are occurring without immediate abiotic assembly into p-TEP. This suggestion is further supported by the statistical relationships between biopolymers and p-TEP and c-TEP which are statistically significant in all of the offshore profiles. There is usually no statistical relationship of significance between p-TEP and c-TEP.

A considerable amount of additional research will be required to better establish the processes occurring within the Red Sea water column that relate to NOM production and transport and how these processes relate to the measured TEP and NOM fraction concentrations. Since there are few data available in the literature that relate these parameters within the water column at other geographic locations, it is difficult to provide definitive conclusions. The data provided herein appear to be the first published that relate the biopolymer fraction of NOM to TEP and provide all of the five fractions of NOM in the offshore marine environment

throughout the water column. The carbon compounds that occur in p-TEP are largely contained within the biopolymer fraction of NOM with the exception of some proteins which occur in the size range found in the humic substances.

4.7. Comparison of the offshore and onshore TEP data in the Red Sea

All of the onshore measurements of p-TEP and c-TEP were collected between the sea surface and a depth of 10 m [9–18]. Therefore, only the data in this depth range can be compared to the offshore data. The full range of p-TEP in the nearshore measurements is from 53 to 347 $\mu\text{g Xeq/L}$ and the c-TEP range is between 36 and 287 $\mu\text{g Xeq/L}$. The ranges in the offshore profiles in the same depth range for p-TEP and c-TEP are 135.4–279.4 and 0–340.7, respectively. In both locations, there was considerable variation between sites and in different times of the year which is expected based on production variations of TEP by algae and bacteria in the upper photic zone as well as the ability of TEP to have either negative or positive buoyancy at shallow depths [21,30,31,43,60].

4.8. Comparison of TEP profiles in the Red Sea with other marine environments

Most TEP data profiles collected in the marine environment show an irregular variation in the upper 100 m of the water column [43,60], a general reduction of TEP with depth over 200 m [37,61], but in some cases an increase at greater depths [62]. Also, the reported changes in TEP with depth are based mostly on p-TEP data and not both types of TEP which show differing trends in the water column. The TEP data collected from the profiles in this investigation within the photic zone (<100 m) show differing concentrations with depth (Figs. 7 and 8). Within the upper 90, p-TEP declines between 31% and 46% at sites A, B, and C and shows no decline in the deep profile. The c-TEP concentration declines between 38% and 70% at sites A, B, and the deep profile, but increases by 150% at site C. For comparison, the TOC concentration reduction in the photic zone ranges between 4% and 32%. In the deep profile the difference between the surface and the 300 m depth showed a reduction in p-TEP of 20% and c-TEP of 69%. This may indicate that some abiotic assembly of p-TEP is occurring below the photic zone, particularly in the presence of bacteria which may feed upon the p-TEP. The TOC in the deep profile declines by about 32% comparing the surface to the 300 m depth.

Table 3
Correlation matrix

	P-TEP ($\mu\text{g Xeq/L}$)	C-TEP ($\mu\text{g Xeq/L}$)	Bacterial count (cells/mL)	Total algae (events/mL)	TOC (mg/L)	Biopolymers
P-TEP ($\mu\text{g Xeq/L}$)	1.000					
C-TEP ($\mu\text{g Xeq/L}$)	0.327	1.000				
Bacteria (cells/mL)	0.152	0.075	1.000			
Algae (events/mL)	0.320	-0.019	0.016	1.000		
TOC (mg/L)	0.259	0.422	0.374	-0.169	1.000	
Biopolymers	-0.263	0.207	-0.006	-0.304	0.209	1.000

4.9. Relationships between NOM fractions and other parameters

The primary fraction of NOM that shows a trend with depth is the biopolymers which track well to bacteria. Since the biopolymer fraction of NOM contains most of the polysaccharides, which can be food for bacteria, the relationship with the bacteria is to be expected. In the upper 100 m of the water column, the humic substances show a restricted range in concentrations with a small downward trend (Fig. 7), but below 100 m there is a lowering concentration following the same pattern as the biopolymers. The building blocks have a larger range in concentration change in the upper 100 m of the water column compared to the humic substances (Fig. 7) and a similar downward trend in concentration similar to the humic substances below 100 m (Fig. 8). The LMW neutrals and acids show considerable variation in concentration in the upper 100 m and a slight downward change in concentration below 100 m.

There are some general suggestions made by these data related to the concentration changes. In the photic zone, the biochemical activity of algae and bacteria affect the NOM fraction concentrations. The LMW fractions are likely affected by the biochemical breakdown of large molecular weight organics and by selective, abiotic aggradation of larger organic particles suggested by the larger concentration of the neutrals over the acids. The reduction in concentrations of biopolymers, humic substances, and building blocks below 100 m follows the reduction in bacteria below the photic zone. As bacteria feed on p-TEP, they may leave behind the LMW neutrals which could be compounds that

cannot be used by the bacteria as food. The LMW acids may tend to occur within the context of c-TEP and may be subject to abiotic aggradation during settling. Future research will be required to understand the complex relations between the NOM organic fractions and the biochemistry of the bacteria in the deep-water column.

4.10. Implications of the Red Sea TEP and bacteria on SWRO desalination

The concentrations of p-TEP onshore at the intakes of various SWRO plants average about 199 $\mu\text{g Xeq/L}$ versus about 200 $\mu\text{g Xeq/L}$ at surface offshore. In the deep profile TEP decreases to about 175 $\mu\text{g Xeq/L}$ at a depth of 220 m and remains nearly constant to 300 m below surface. Therefore, the pretreatment processes for seawater intakes onshore and offshore have about equivalent challenges. The p-TEP in the shallow offshore profiles averages close to 120 $\mu\text{g Xeq/L}$ at 90 m and in the deep profile averages 170 $\mu\text{g Xeq/L}$ at depths from 220 to 300 m. Therefore, deep water intakes would yield little advantage over shallow intakes if the deep water intake were technically feasible. Dehwah et al. [11] found that the cliffed area beyond the reef tract along the Red Sea margin made deep intakes to greater than 100 m not feasible. Water depth increases from 20 m to over 600 m in a horizontal distance of less than 100 m. A deep intake would have to be hung on the cliff. Since this area is subject to earthquakes, this type of intake cannot be safely used.

Bacteria concentrations at the SWRO intakes (Table 1) were 638,822 cells/mL compared to near 500,000 cells/mL

Table 4
Multiple Regression analysis of selected organic parameters at the 0.05 significance level

Dependent variable	Location	Attributes	P-value	R-square	Adjusted R-square	Overall significance
p-TEP	Offshore	Bacterial count (cells/mL)	0.00106	0.51941	0.48874	0.0000001
		Total algae (events/mL)	0.00127			
		TOC (mg/L)	0.76006			
	Nearshore	Bacterial count (cells/mL)	0.48082			
		Total algae (events/mL)	0.15212			
		TOC (mg/L)	0.37855			
c-TEP	Offshore	Bacterial count (cells/mL)	0.91115	0.13834	0.01525	0.36195
		Total algae (events/mL)	0.93401			
		TOC (mg/L)	0.00540			
	Nearshore	Bacterial count (cells/mL)	0.88360			
		Total algae (events/mL)	0.37529			
		TOC (mg/L)	0.18425			
c-TEP	Offshore	p-TEP ($\mu\text{g Xeq/L}$)	0.00750	0.13704	0.11943	0.00750
	Nearshore	p-TEP ($\mu\text{g Xeq/L}$)	0.06876	0.14271	0.10374	0.06876
		Bacterial count (cells/mL)	0.00296			
Biopolymers	Offshore	P-TEP ($\mu\text{g Xeq/L}$)	0.00001	0.36179	0.32106	0.00009
		C-TEP ($\mu\text{g Xeq/L}$)	0.03707			
		Bacterial count (cells/mL)	0.07978			
	Nearshore	Total algae (events/mL)	0.51524			
		P-TEP ($\mu\text{g Xeq/L}$)	0.38547			
		C-TEP ($\mu\text{g Xeq/L}$)	0.34150			

at the surface offshore. This is considered to be a minor difference with regard to the pretreatment design to reduce concentrations in an SWRO facility. There are substantial declines in bacteria concentrations with depth offshore which would aid pretreatment processes in SWRO plants. However, the use of deep intakes at 100 to 150 m is still not technically feasible [11].

5. Conclusions

Vertical changes in concentrations of TEP in the Red Sea tend to follow trends found in other locations of the world ocean in that there is a general reduction with depth. The changes in the photic zone tend to be quite irregular, as expected, because of variations in primary productivity and differing biochemical conditions. Although it was observed that no clear relationship between TEP and algae occurs in the Red Sea, this unusual result may be explained by the dominance of small algae and cyanobacteria.

The measurement of the five fractions of NOM allows some preliminary conclusions to be made concerning the relationships between specific organic parameters and TEP variation with depth. These relationships suggest that extracellular discharges of polysaccharides and proteins from the bacteria and algae are occurring without immediate abiotic assembly into p-TEP in the photic zone of the water column. In the water column below the photic zone, TOC, bacteria, and biopolymers show a generally common rate of reduction in concentration, but p-TEP concentration changes at a reduced rate showing that it persists in moving organic carbon deeper into the water column despite consumption by bacteria. There may be some abiotic assembly of c-TEP into p-TEP to maintain the concentration without full bacterial removal.

The multiple regression analysis showed that p-TEP is correlated with bacteria and algae offshore, but no statistical correlation occurs between these variables in the nearshore data. No statistical correlation occurs between c-TEP and bacteria, algae, and TOC in offshore and nearshore samples. Also, p-TEP and c-TEP are not statistically correlated. The concentrations of biopolymers is correlated to bacteria, p-TEP, and c-TEP in the offshore samples, but not on the onshore samples.

The relationships between p-TEP and c-TEP and other organic parameters, especially the biopolymer fraction of NOM, is different when comparing the offshore water column to the nearshore area. Seasonal differences during sampling could have also impacted the results. Differences in local conditions, such as circulation and anthropogenic influences, in the nearshore zone can cause large variations in the organic parameters measured, not allowing statistically-significant relationships to be established.

Comparisons of some key parameters that can indicate biofouling potential (p-TEP and bacteria concentrations) show that SWRO treatment of seawater taken from nearshore and offshore intakes would present equal challenges for removal in pretreatment processes. The p-TEP shows some minor declines and bacteria concentration decrease significantly offshore. However, the use of deep water intakes along the Red Sea margin is not technically feasible due to the cliffs that occur seaward of the reefs.

Acknowledgments

Funding for the offshore sample collection was provided by the King Abdullah University of Science and Technology, Coastal and Marine Resources Core Laboratory. Analytical work was funded by the Water Desalination and Reuse Center, King Abdullah University of Science and Technology. Support for DMA was provided by the National Science Foundation (Grants OCE-0850421 OCE-0430724, OCE-0911031, and OCE-1314642) and National Institutes of Health (NIEHS-1P50-ES021923-01) through the Woods Hole Center for Oceans and Human Health.

References

- [1] H.C. Flemming, G. Schaule, T. Griebel, J. Schmitt, A. Tamachkiarowa, Biofouling – the Achilles heel of membrane processes, *Desalination*, 113 (1997) 215–225.
- [2] J.S. Baker, L.Y. Dudley, Biofouling in membrane systems – a review, *Desalination*, 118 (1998) 81–90.
- [3] T. Nguyen, F.A. Roddick, L. Fan, Biofouling of water treatment membranes: a review of the underlying causes, monitoring techniques and control measures, *Membranes (Basel)*, 2 (2012) 804–840.
- [4] H. Winters, T.H. Chong, A.G. Fane, W. Krantz, M. Rzechowicz, N. Saeidi, The involvement of lectins and lectin-like humic substances in biofilm formation – is TEP important?, *Desalination*, 399 (2016) 61–68.
- [5] T. Berman, M. Holenberg, Don't fall foul of biofilm through high TEP levels, *Filtr. Sep.*, 42 (2005) 30–32.
- [6] L.O. Villacorte, M.D. Kennedy, G.L. Amy, J.C. Schippers, Measuring transparent exopolymer particles (TEP) as indicator of the (bio)fouling potential of RO feed water, *Desal. Water Treat.*, 5 (2009) 207–212.
- [7] T. Berman, Transparent exopolymer particles as critical agents in aquatic biofilm formation: implications for desalination and water treatment, *Desal. Water Treat.*, 51 (2013) 1014–1020.
- [8] E. Bar-Zeev, U. Passow, C.S. Romero-Vergas, M. Elimelech, Transparent exopolymer particles (TEP): from aquatic environments and engineered systems to membrane biofouling, *Environ. Sci. Technol.*, 49 (2015) 691–707.
- [9] A.H.A. Dehwah, S. Al-Mashharawi, N. Kammourie, T.M. Missimer, Impact of well intake systems on bacterial, algae and organic carbon reduction in SWRO desalination systems, *SAWACO, Jeddah, Saudi Arabia, Desal. Water Treat.*, 55 (2015) 2594–2600.
- [10] A.H.A. Dehwah, S. Li, S. Al-Mashhaarwi, H. Winters, T.M. Missimer, Changes in feedwater organic matter concentrations based on intake type and pretreatment processes at SWRO facilities, Red Sea, Saudi Arabia, *Desalination*, 360 (2015) 19–27.
- [11] A.H.A. Dehwah, S. Li, S. Al-Mashharawi, F.L. Mallon, Z. Batang, T.M. Missimer, Effects of Intake Depth on Raw Seawater Quality in the Red Sea, T.M. Missimer, B. Jones, R.G. Maliva, Eds., *Intakes and Outfalls for Seawater Reverse Osmosis Desalination Facilities: Innovations and Environmental Impacts*, Springer, Berlin, 2015, pp. 105–124.
- [12] A.H.A. Dehwah, T.M. Missimer, Subsurface intake systems: green choice for improving feed Seawater quality at SWRO desalination plants, Jeddah, Saudi Arabia, *Water Res.*, 88 (2016) 216–224.
- [13] R.M. Rachman, S. Li, T.M. Missimer, SWRO feed water quality improvement using subsurface intakes in Oman, Spain, Turks and Caicos Islands, and Saudi Arabia, *Desalination*, 351 (2014) 88–100.
- [14] R.M. Rachman, A.H.A. Dehwah, S. Li, H. Winters, S. Al-Mashharawi, T.M. Missimer, Effects of Well Intake Systems on Removal of Algae, Bacteria, and Natural Organic Matter, T.M. Missimer, B. Jones, R.G. Maliva, Eds., *Intakes and Outfalls for Seawater Reverse Osmosis Desalination Facilities: Innovations and Environmental Impacts*, Springer, Berlin, 2015, pp. 163–193.

- [15] A.H. Alshahri, A.H.A. Dehwah, T. Leiknes, T.M. Missimer, Organic carbon movement through two SWRO facilities from source water to pretreatment to product with relevance to biofouling, *Desalination*, 407 (2017) 52–60.
- [16] A.H.A. Dehwah, S. Al-Mashharawi, K.C. Ng, T.M. Missimer, Aquifer treatment of seawater to remove natural organic matter before desalination, *Ground Water*, 55 (2016) 316–326.
- [17] A.H.A. Dehwah, T.M. Missimer, Seabed gallery intakes: investigation of the water pretreatment effectiveness of the active layer using a long-term column experiment, *Water Res.*, 121 (2017) 95–108.
- [18] A.H.A. Dehwah, T.M. Missimer, Regrowth of Bacteria and TEP Production in Cartridge Filters: Are Cartridge Filter Necessary in Some SWRO Plants?, In: *Proceedings, American Membrane Technology Association/American Water Works Association, 2015 Membrane Technology Conference and Exposition, Orlando, FL, 2015*.
- [19] F. Azam, F. Malfatti, Microbial structuring of marine ecosystems, *Nat. Rev. Microbiol.*, 5 (2007) 782–791.
- [20] A.L. Alldredge, K.M. Croker, Why do sinking mucilage aggregates accumulate in the water column?, *Sci. Total Environ.*, 165 (1995) 15–22.
- [21] U. Passow, Transparent exopolymer particles (TEP) in aquatic environments, *Prog. Oceanogr.*, 55 (2002) 287–333.
- [22] U. Passow, R.F. Shipe, A. Muarry, D.K. Pak, M.A. Brzezinski, A.L. Alldredge, The origin of transparent exopolymer particles (TEP) and their role in the sedimentation of particulate matter, *Cont. Shelf Res.*, 21 (2001) 327–346.
- [23] O. Wurl, L. Miller, S. Vagle, Production and fate of transparent exopolymer particles in the ocean, *J. Geophys. Res.*, 116 (2001) 1–16.
- [24] P. Verdugo, A.L. Alldredge, F. Azam, D.L. Kirchman, U. Passow, P.H. Santschi, The oceanic gel phase: a bridge in the DOM-POM continuum, *Mar. Chem.*, 92 (2004) 67–85.
- [25] M. Bižić-Ionescu, D. Ionescu, H.P. Grossart, Organic particles: heterogeneous hubs for microbial interactions in aquatic ecosystems, *Front. Microbiol.*, 9 (2018) 2569.
- [26] W.-C. Chin, M.V. Orellana, P. Werdugo, Spontaneous assembly of marine dissolved organic matter in polymer gels, *Nature*, 391 (1998) 568–572.
- [27] K.E. Stoderegger, G.J. Herndl, Production of exopolymer particles of marine bacterioplankton under contrasting turbulence conditions, *Mar. Ecol. Prog. Ser.*, 189 (1999) 9–16.
- [28] T. Berman, Y. Viner-Mozzini, Abundance and characteristics of polysaccharide and proteinaceous particles in Lake Kinneret, *Aquat. Microb. Ecol.*, 24 (2001) 255–264.
- [29] U. Passow, A.L. Alldredge, B.F. Logan, The role of particulate carbohydrates in the flocculation of diatom blooms, *Deep Sea Res. Part I*, 41 (1994) 335–357.
- [30] J. Zhou, K. Mopper, U. Passow, The role of surface-active carbohydrates in the formation of transparent exopolymer particulates by bubble adsorption of seawater, *Limnol. Oceanogr.*, 43 (1998) 1860–1871.
- [31] X. Mari, F. Rassoulzadegan, C.P.D. Brussaard, Role of TEP in the microbial food web structure. II. Influence of the ciliate community structure, *Mar. Ecol. Prog. Ser.*, 279 (2004) 23–32.
- [32] F. Azam, R.A. Long, Sea snow microcosms, *Nature*, 414 (1995) 495–497.
- [33] A. Engel, S. Thoms, U. Rieesell, E. Rochelle-Newall, I. Zondervan, Polysaccharide aggregation as a potential sink of marine dissolved organic carbon, *Nature*, 428 (2004) 929–932.
- [34] K. Azetsu-Scott, U. Passow, Ascending marine particles: significance of transparent exopolymer particles (TEP) in the upper ocean, *Limnol. Oceanogr.*, 49 (2004) 741–748.
- [35] O.L. Wurl, M. Holmes, The gelatinous nature of the sea-surface microlayer, *Mar. Chem.*, 100 (2008) 89–97.
- [36] O. Wurl, L. Miller, R. Röttgers, S. Vagle, The distribution and fate of surface-active substances in the sea-surface microlayer and water column, *Mar. Chem.*, 115 (2009) 1–9.
- [37] M.K. Jennings, U. Passow, A.S. Wozinak, D.A. Hansell, Distribution of transparent exopolymer particles (TEO) across an organic carbon gradient in the western North Atlantic Ocean, *Mar. Chem.*, 190 (2017) 1–12.
- [38] A. Engel, Distribution of transparent exopolymer particles (TEP) in the northeast Atlantic Ocean and their potential significance for aggregation processes, *Deep Sea Res. Part I*, 51 (2004) 83–92.
- [39] M. Simon, H.P. Grossart, B. Schweitzer, H. Ploug, Microbial ecology of organic aggregates in aquatic ecosystems, *Aquat. Microb. Ecol.*, 28 (2002) 175–211.
- [40] E. Ortega-Retuerta, I. Reche, E. Pulido-Villena, Agustí S, Duarte CM, Uncoupled distributions of transparent exopolymer particles (TEP) and dissolved carbohydrates in the Southern Ocean, *Mar. Chem.*, 115 (2009) 59–65.
- [41] E. Ortega-Retuerta, C.M. Duarte, I. Reche, Significance of bacterial activity for the distribution and dynamics of transparent exopolymer particles in the Mediterranean Sea, *Microb. Ecol.*, 59 (2010) 808–818.
- [42] E. Bar-Zeev, T. Berman, E. Rahav, G. Dishon, B. Herut, N. Kress, I. Berman-Frank, Transparent exopolymer particle (TEP) dynamics in the eastern Mediterranean Sea, *Mar. Ecol. Prog. Ser.*, 431 (2011) 107–118.
- [43] E. Ortega-Retuerta, M.M. Sala, E. Borrull, M. Mestre, F.L. Aparicio, R. Gallisai, C. Antequera, C. Marrasé, F. Peters, R. Simó, J.M. Gasol, Horizontal and vertical distributions of transparent exopolymer particles (TEP) in the NW Mediterranean Sea are linked to chlorophyll A and O₂ variability, *Front. Microbiol.*, 7 (2017) 2159.
- [44] E.I. Bar-Zeev, I. Berman-Frank, B. Liberman, E. Rahav, U. Passow, T. Berman, Transparent exopolymer particles: potential agents for organic fouling and biofilm formation in desalination and water treatment plants, *Desal. Water Treat.*, 3 (2009) 136–142.
- [45] E.I. Bar-Zeev, I. Berman-Frank, N. Stambler, E.V. Domínguez, T. Zohary, E. Capuzzo, E. Meeder, D.J. Sugget, D. Iluz, G. Dishon, T. Berman, Transparent exopolymer particles (TEP) link phytoplankton and bacterial production in the Gulf of Aqaba, *Aquat. Microb. Ecol.*, 56 (2009) 217–226.
- [46] R. Van der Merwe, F. Hammes, S. Lattemann, G. Amy, Flow cytometric assessment of microbial abundance in the near-field area of seawater reverse osmosis concentrate discharge, *Desalination*, 343 (2014) 208–216.
- [47] J. Vives-Rego, P. Lebaron, G. Nebe-von Caron, Current and future applications of flow cytometry in aquatic microbiology, *FEMS Microbiol. Rev.*, 24 (2000) 429–448.
- [48] R. Tomisalv, T. Šilović, D. Šantić, D. Fuks, M. Mičić, Preliminary flow cytometric analysis of phototrophic picoplankton communities in the Northern Adriatic, *Fresenius Environ. Bull.*, 18 (2009) 715–724.
- [49] S.A. Huber, A. Balz, M. Abert, W. Pronk, Characterization of aquatic humic and non-humic matter with size-exclusion chromatography-organic carbon detection-organic nitrogen detection (LC-OCD-OND), *Water Res.*, 45 (2011) 879–885.
- [50] U. Passow, A.L. Alldredge, A dye-binding assay for spectrophotometric measurement of transparent exopolymer particles (TEP), *Limnol. Oceanogr.*, 40 (1995) 1326–1335.
- [51] Y. Chen, G. Dong, J. Han, B.W. Wah, J. Wang, Multi-Dimensional Regression Analysis of Time-Series Data Streams, In: *Proceedings of the 28th VLDB International Conference on Very Large Databases, Hong Kong, China, 2002*, pp. 323–334.
- [52] S. Tonidandel, J.M. LeBreton, Relative importance analysis: a useful supplement to regression analysis, *J. Bus. Psychol.*, 26 (2011) 1–9.
- [53] J. Osborne, E. Waters, Four assumptions of multiple regression that researchers should always test, *Pract. Assess. Res. Eval.*, 8 (2002) 1–9.
- [54] M.N. Williams, C.A. Grajales, D. Kurkiewicz, Assumptions of multiple regression: correcting two misconceptions, *Pract. Assess. Res. Eval.*, 18 (2013) 1–13.
- [55] D. Lindell, A.F. Post, Ultraphytoplankton succession is triggered by deep winter mixing in the Gulf of Aqaba (Eilat), Red Sea, *Limnol. Oceanogr.*, 40 (1995) 1130–1141.
- [56] G. Yahel, A.F. Post, K. Fabricius, D. Marie, D. Vaultot, A. Genin, Phytoplankton distribution and grazing near coral reefs, *Limnol. Oceanogr.*, 43 (1998) 551–563.
- [57] U. Sommer, Scarcity of medium-sized phytoplankton in the northern Red Sea explained by string bottom-up and weak top-down control, *Mar. Ecol. Prog. Ser.*, 197 (2000) 19–25.

- [58] B. Kimor, B. Goldanski, Microplankton of the Gulf of Elat: aspects of seasonal and bathymetric distribution, *Mar. Biol.*, 41 (1992) 55–67.
- [59] F. Iuculano, I.P. Mazuecos, I. Reche, S. Agusti, *Prochlorococcus* as a possible source for transparent exopolymer particules (TEP), *Front. Microbiol.*, 8 (2017) 709.
- [60] S. Schuster, G.J. Herndl, Formation and significance of transparent exopolymer particles in the northern Adriatic Sea, *Mar. Ecol. Prog. Ser.*, 124 (1995) 227–236.
- [61] K. Busch, S. Endreas, M.H. Iverson, J. Michels, E.-M. Nöthig, A. Engel, Bacterial colonization and vertical distribution of marine gel particles (TEP and CSP) in the Arctic Fram Strait, *Front. Mar. Sci.*, 4 (2017) 166.
- [62] N. Ramaiah, V.V.S.S. Sarma, M. Gauns, M. Dileep Kumar, M. Madhupratap, Abundance and relationship of bacteria with transparent exopolymers during the 1996 summer monsoon in the Arabian Sea, *J. Earth Syst. Sci.*, 109 (2000) 443–451.